



Mapping Complex Landslide Scars Using Deep Learning and High-Resolution Topographic Derivatives from LiDAR Data in Quebec, Canada

Hejar Shahabi, Saeid Homayouni, Didier Perret & Bernard Giroux

To cite this article: Hejar Shahabi, Saeid Homayouni, Didier Perret & Bernard Giroux (2024) Mapping Complex Landslide Scars Using Deep Learning and High-Resolution Topographic Derivatives from LiDAR Data in Quebec, Canada, Canadian Journal of Remote Sensing, 50:1, 2418087, DOI: [10.1080/07038992.2024.2418087](https://doi.org/10.1080/07038992.2024.2418087)

To link to this article: <https://doi.org/10.1080/07038992.2024.2418087>



© 2024 The Author(s). Published by Informa UK Limited, trading as Taylor & Francis Group.



Published online: 25 Oct 2024.



Submit your article to this journal [↗](#)



Article views: 147



View related articles [↗](#)



View Crossmark data [↗](#)

Mapping Complex Landslide Scars Using Deep Learning and High-Resolution Topographic Derivatives from LiDAR Data in Quebec, Canada

Hejar Shahabi^a, Saeid Homayouni^a, Didier Perret^b, and Bernard Giroux^a

^aCentre Eau Terre Environnement, Institut National de la Recherche Scientifique (INRS), Québec City, Canada; ^bGeological Survey of Canada, Natural Resources Canada, Québec City, Canada

ABSTRACT

This study evaluates deep learning (DL) models, particularly ResU-Net with attention mechanisms, for mapping landslides in Quebec, Canada, utilizing high-resolution digital elevation model (HRDEM) data and its seven derivatives (slope, aspect, hillshade, curvature, ruggedness, surface area ratio, and max difference from mean). Three scenarios were considered to assess the effectiveness of various features in landslide segmentation: training the model on all features, each feature individually, and on slope and hillshade. Model performance on individual features was significantly poor, while the model trained with hillshade and slope outperformed the model using all seven features, particularly in F1-score (improved by 8% for rotational landslides and 11% for retrogressive landslides) during validation. Furthermore, for the test dataset, model performance on all seven features was compared against slope and hillshade. As a result, for rotational landslides, slope and hillshade achieved F1-scores of 0.68 and 0.93 for rotational and retrogressive landslides, respectively, while the same metrics using all features were 0.61 and 0.83, respectively. This suggests hillshade and slope provide the most relevant information and reduce computational complexity. Overall, the findings enhance our understanding of HRDEM derivatives and emphasize the importance of feature selection in optimizing model performance and reducing computational complexity.

ARTICLE HISTORY

Received 2 July 2024
Accepted 13 October 2024

KEYWORDS



Remote sensing; rotational landslide; retrogressive landslide; machine learning

Introduction

A landslide involves the downward sliding of a large number of rocks, debris, or soil along a slope. It is a type of natural hazard that poses a significant threat to human life, natural resources, infrastructure, and properties in various forms (Guzzetti, 2000; Shahabi et al., 2021; Varnes, 1978). In Canada, thousands of landslides occur each year, and those that are small or occur in remote areas remain mostly unnoticed. Since 1771, landslides and avalanches have killed more than 700 people and have cost Canadians billions of dollars – with annual costs reaching approximately \$200 - 400 million (Blais-Stevens et al., 2018; Chapuis, 2016). In Quebec province, large destructive landslides have mostly occurred in sensitive clay soils, and their spatial extent ranges from a few meters to hundreds of meters (Locat et al., 2011; Poulin Leboeuf, 2020). Such large landslides, also known as Retrogressive

landslides, occur in the clayey soils deposited in the postglacial seas of Québec, and the province is significantly exposed to this type of hazard. Any efforts to mitigate landslide risks must start with an inventory (Guzzetti et al., 2012). In this regard, visually interpreting aerial or very high-resolution (VHR) satellite images is still the most common procedure for landslide mapping. However, several drawbacks are associated with this approach: multi-temporal analysis of large areas is time-consuming and difficult to implement. Moreover, the effectiveness of the produced landslide maps is influenced by factors such as the expertise of the researcher, the intended use of the maps, their scale, and the data employed in their creation.

In contrast, remote sensing (RS) techniques have opened a new era, particularly for mapping natural hazards in difficult-access or remote areas (Hölbling et al., 2016). However, for images with intricate

CONTACT Hejar Shahabi  hejar.shahabi@inrs.ca  Institut National de la Recherche Scientifique (INRS), 490 Couronne St, Québec City, QC G1K 9A9, Canada

© 2024 The Author(s). Published by Informa UK Limited, trading as Taylor & Francis Group.
This is an Open Access article distributed under the terms of the Creative Commons Attribution License (<http://creativecommons.org/licenses/by/4.0/>), which permits unrestricted use, distribution, and reproduction in any medium, provided the original work is properly cited. The terms on which this article has been published allow the posting of the Accepted Manuscript in a repository by the author(s) or with their consent.

textures and intensive spectral heterogeneity, conventional models such as Parallelepiped and Maximum Likelihood fail for image classification; thus, advanced ML models, including Logistic Regression (LG), Decision Tree (DT), K-Nearest Neighbor (KNN), Support Vector Machine (SVM), Artificial Neural Network (ANN), Random Forest (RF) and extreme gradient boosting (XGBoost) are applied to address these issues (Ma et al., 2019; Shih et al., 2019). Object-based image analysis (OBIA) has emerged as a new paradigm for addressing issues associated with the pixel-based approach. OBIA is a knowledge-driven approach that imitates human perception to group a set of similar pixels into meaningful objects through an image segmentation procedure that fairly represents corresponding features in the real world (Shahabi et al., 2019; Tavakkoli Piralilou et al., 2019). In this regard, several studies (Azhand et al., 2024; Ghorbanzadeh et al., 2022, 2023; Hölbling et al., 2015; Ju et al., 2022; Keyport et al., 2018; Saba et al., 2023; Shahabi et al., 2019; Tavakkoli Piralilou et al., 2019) have shown that using OBIA to automatically extract landslide inventory scars is superior to pixel-based. Advancements in the field of computer vision and graphics processing units (GPUs) have provided researchers with opportunities to explore Deep Learning (DL) techniques for many intricate tasks, particularly natural language processing (NLP) and computer vision applications like image classification and object detection (Ghorbanzadeh et al., 2021, 2022, 2024; Lu et al., 2023; Mohan et al., 2021; Prakash et al., 2020; Shahabi et al., 2024).

In computer vision, specialized models like AlexNet, VGG Net, GoogleNet, ResNet, and DenseNet have been specifically designed to address challenges in image classification (Mohan et al., 2021). However, within remote sensing (RS), particularly for tasks like image classification, the objective is to assign labels to every pixel in an image. Deep Learning semantic segmentation techniques such as the Fully Convolutional Network (FCN) are applied (Maggiori et al., 2016). The U-net model (Ronneberger et al., 2015), an enhancement over FCN utilizing encoder-decoder architectures, has gained widespread popularity in tasks like image segmentation and object detection despite its initial design for medical image segmentation (Ghorbanzadeh et al., 2021). Additionally, region-based models like Faster R-CNN (Tanatipuknon et al., 2021) and Mask R-CNN (He et al., 2017; Ullo et al., 2021) have been developed for object detection and segmentation. More recently, transformers have demonstrated success in remote sensing applications (Aleissae et al., 2023), notably in tasks like landslide inventory (Tang

et al., 2022; Wang et al., 2022). Nevertheless, the prevailing trend involves implementing such algorithms primarily on multispectral RS data. In contrast, our situation relies solely on an elevation dataset, and models tailored for such specific scenarios are not widely available (Chen et al., 2014; Fang et al., 2022; Li et al., 2015; Mezaal et al., 2018; Pawłuszek et al., 2019).

To the best of our knowledge, there is a dearth of studies exploring the use of DL models for mapping landslides in the Quebec province, particularly in leveraging elevation data and its derivatives. Consequently, the objectives of this study are to pioneer the development and assessment of a DL model tailored for mapping complex landslide scars across selected sites in the southern regions of Quebec and find the suitable high-resolution digital elevation model (HRDEM) derivatives to detect landslide scars using DL. This endeavor is grounded in utilizing publicly accessible elevation data provided by the provincial government (Natural Resources Canada 2019).

Study area and data

Study area

This research focuses on the southern region of Quebec, Canada, which is particularly susceptible to landslides due to its unique geological, geomorphological, and climatic characteristics. This area, encompassing the St. Lawrence Lowlands, Saguenay-Lac-Saint-Jean region, and the Ottawa Valley, is characterized by the presence of sensitive clay soils, which can rapidly transform from a solid to a fluid state when disturbed (L'Heureux et al., 2014). The region's topography varies from gentle slopes to more pronounced elevations, creating diverse conditions for landslide occurrence such as Retrogressive landslides in sensitive clays. Such landslides are most generally located along river or stream valleys and can start with an initial Rotational slide along a slope, which may be triggered by factors like riverbank erosion, excavation at the base of the slope, excess weight at or near the top of the slope, rising porewater pressures due to rainfall or snowmelt, or seismic activity (Locat et al., 2011; Perret et al., 2019). Retrogressive landslides can be grouped into two main types depending on the failure mode: spreads and flows (Perret et al., 2019), which are particularly dangerous because they can occur very rapidly, in a few minutes, often without obvious warning signs and can travel significant distances, sometimes exceeding a few hundred meters.

Rotational landslides, another type of landslide observed in the region (Poulin Leboeuf, 2020), involve the downward and outward movement of soil along a concave-upward failure surface. These landslides typically occur in homogeneous materials and are characterized by a Rotational movement around an axis parallel to the slope (Azañón et al., 2005; Ma et al., 2023). The combination of sensitive clay soils and the region's topography makes southern Quebec particularly vulnerable to both Retrogressive and Rotational landslides since most of Quebec's population resides within the marine limits of the ancient Champlain, Laflamme, and Goldthwaite seas necessitating comprehensive risk assessment and management strategies to mitigate their impact (Figure 1).

Figure 2 shows the four selected sites for Retrogressive and Rotational landslide detection: two for training, one for validation and one for testing.

Topographic and LiDAR dataset

The dataset used in this study comes from HRDEM product generated from airborne LiDAR data, predominantly in the southern regions. The Digital Terrain Model (DTM) and Digital Surface Model (DSM) are the main products derived from LiDAR data. Regarding DTM datasets, the associated information includes a slope, aspect, shaded relief, color

relief, and color-shaded relief maps, while for DSM datasets, the derived data consists of shaded relief, color relief, and color-shaded relief maps. In the southern region, DTM and DSM datasets are available at 1-meter or 2-meter resolutions and are projected onto the UTM NAD83 (CSRS) coordinate system, aligning with the respective zones. Notably, datasets with a 1-meter resolution cover a spatial extent of 10 by 10 km, while datasets with a 2-meter resolution encompass an area of 20 by 20 km. Since the dataset with a 2-meter resolution covered our entire study area, we decided to use a 2-meter HRDEM product. Based on visual Inspection features including Hillshade, Slope, Geomorphon, Total Curvature, Terrain Ruggedness Index (TRI), Surface Area Ratio (SAR), and Max Difference From Mean (MDFM) were the best ones, the display landslides boundary and texture in different setting and regions. Hillshading is a method used to depict terrain by simulating illumination based on the elevation surface's slope and orientation (Gallant, 2000). Using this technique, the three-dimensional appearance of the terrain can be enhanced and generate a 3D representation of the surface, making it easier to identify landscape features. At the same time, the slope is steepness in degrees, radians, or percent for each grid cell in an input digital elevation model (DEM). Geomorphon is a useful technique for representing and classifying landforms based on elevation differences of a grid cell in

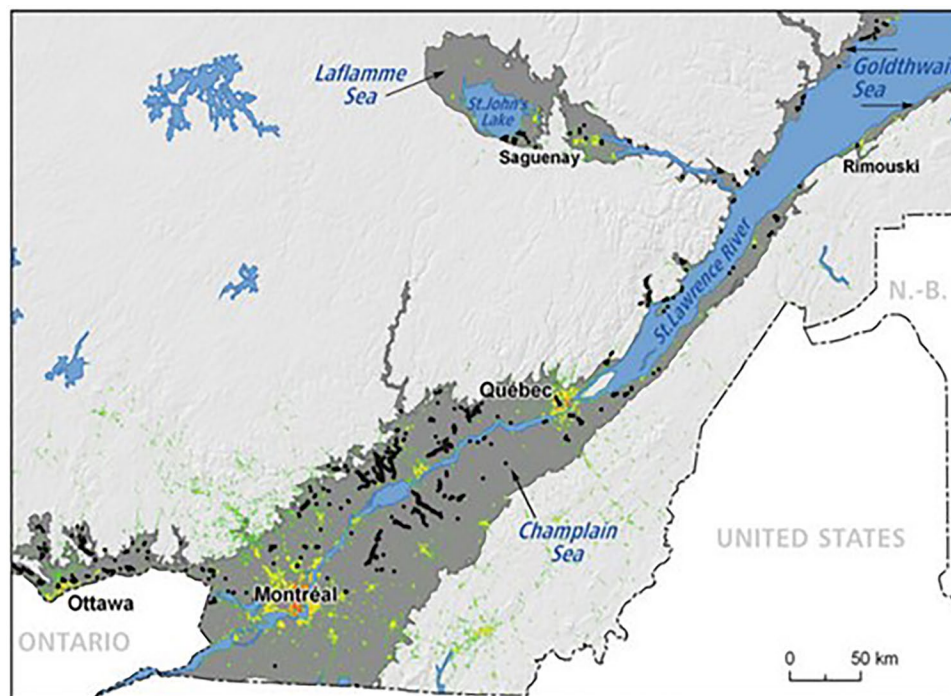


Figure 1. The population heat map (Demers et al., 2017) in southern Quebec's residential areas overlaid on the marine limit. Black dots represent landslide scars.

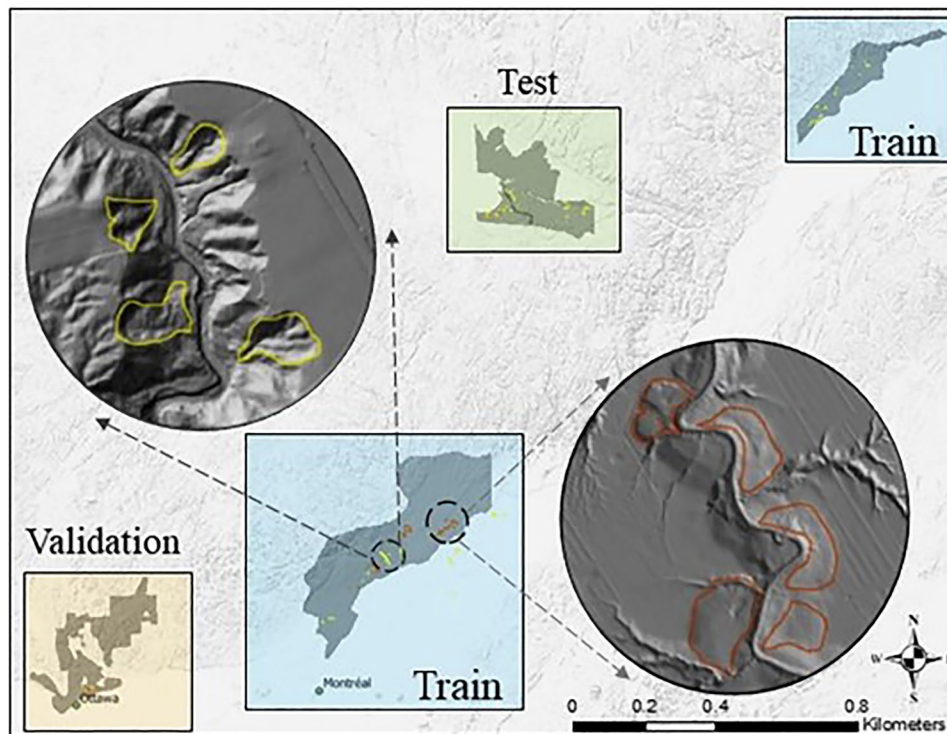


Figure 2. Sites affected by landslide in the southern part of the Quebec province. Yellow and Brown polygons overlaid over Hillshade are selected samples of Rotational and Retrogressive landslides.

a DEM. Line-of-sight analysis for the eight topographic profiles in the cardinal directions surrounding each grid cell in the input DEM is the main concept of Geomorphon. It classifies landforms into 1 to 10 classes, including lat, peak, ridge, shoulder, spur, slope, hollow, footslope, valley, and pit, respectively (Jasiewicz and Stepinski, 2013). Total curvature combines profile and plan curvature, which comprehensively measures how the terrain surface changes in both profile and plan directions (Florinsky, 2016). The curvature value may be positive or negative, and a curvature of zero shows that the surface is either flat or that any convexity in one direction is offset by concavity in another. Total curvature is expressed in units of m^{-1} .

Furthermore, TRI can be applied to highlight the elevation difference between neighboring cells of a DEM (Florinsky, 2016). TRI is calculated by considering the elevation deviations of each pixel from the mean elevation within a defined neighborhood or window. Higher values of TRI indicate more rugged terrain and vice versa. However, SAR estimates the ratio between the surface area and planar area on a terrain or landscape, providing insight into the degree of complexity or irregularity in the land surface (Jenness, 2004). SAR is calculated by considering the terrain's total surface area relative to the same area's horizontal projection. Finally, MDFM is applied to quantify the maximum variation or difference between

elevation values within a given terrain (Lindsay, 2005). This index calculates the largest discrepancy between a specific point's elevation and the surrounding area's mean elevation, often within a defined neighborhood or window. Figure 3 shows an inventory of Retrogressive and Rotational landslide polygons overlaid on topographic features extracted from the DEM.

Methodology

U-Net

U-Net, a FCN model introduced by Ronneberger et al. (2015), has become a standard for image segmentation tasks, particularly in medical image analysis for applications like cell segmentation and tumor detection (Ghorbanzadeh et al., 2021; Kariminejad et al., 2024; Zhang et al., 2018). Its architecture is composed of two main parts: an encoder network that extracts features from the input image through a series of convolutional and max-pooling layers, and a decoder network that reconstructs the segmentation map using upsampling and convolutional layers (Ronneberger et al., 2015). A key feature of U-Net is the use of skip connections that link corresponding layers in the encoder and decoder networks, allowing the decoder to access high-resolution feature maps from the encoder (Ronneberger et al., 2015; Su et al., 2022).

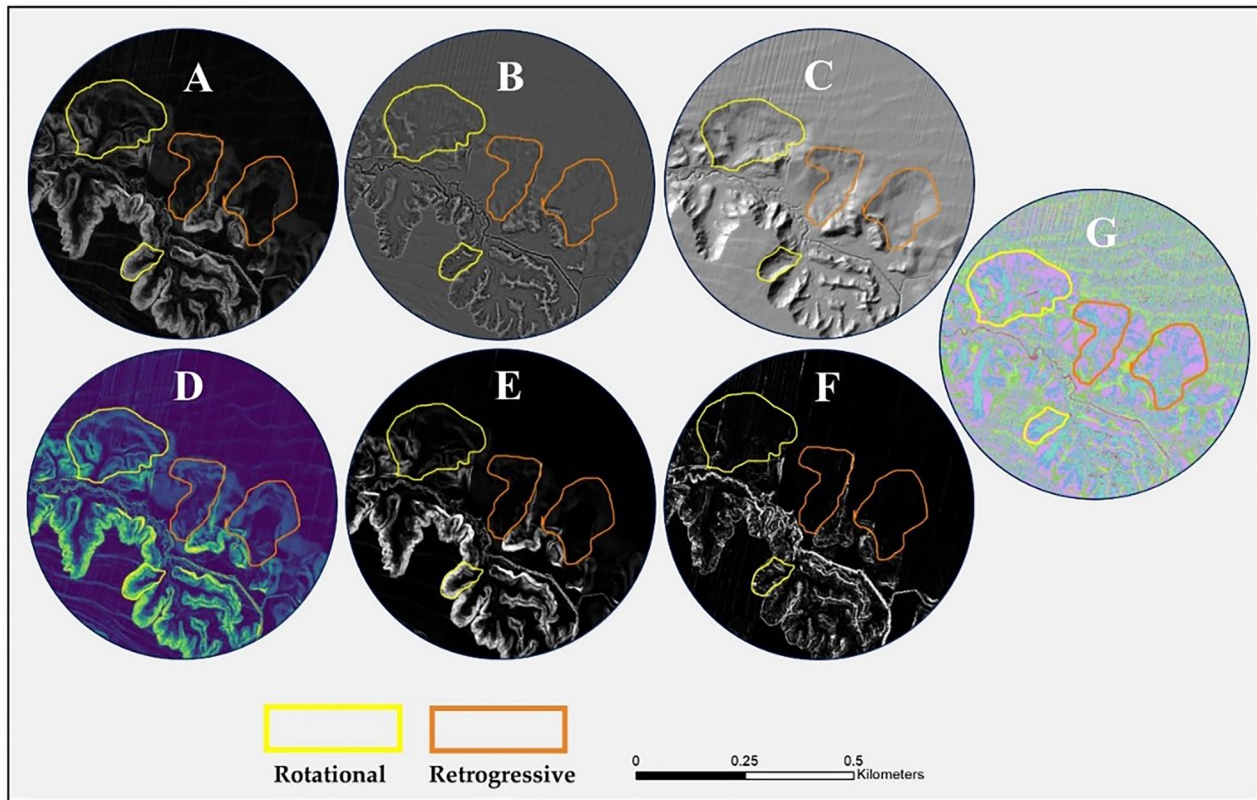


Figure 3. Visual representation of features extracted from DEM. Plots from A to G stand for TRI, MDFM, Hillshade, Slope, SAR, Total Curvature, and Geomorphon features, respectively.

This design helps maintain spatial information, significantly enhancing segmentation accuracy. While U-Net has been successfully adapted for other fields, such as remote sensing image classification, it is not without limitations, including the potential for the vanishing gradient problem, which can hinder its performance in some scenarios.

ResU-Net

In deep learning models, particularly those with significant depth, vanishing gradient problems arise as gradients diminish exponentially during backpropagation, making it challenging for the network to learn meaningful feature representations. This issue is evident in models like U-Net, where training becomes difficult due to minimal updates in the earlier layers. To combat this issue (He et al., 2016) introduced Residual Networks (ResNets), which use residual blocks to overcome the vanishing gradient problem. The core idea behind ResNets is the use of skip or shortcut connections that bypass one or more layers, allowing gradients to flow more effectively from later layers back to the initial layers (He et al., 2016; Yang et al. 2022). Each ResNet layer is composed of multiple blocks, featuring convolution, batch normalization, and ReLU activation functions, which enable the

construction of deeper networks without suffering from gradient issues. Various ResNet variants, such as ResNet-18, ResNet-34, ResNet-50, ResNet-101, and ResNet-152, have been developed, with ResNet-50 being particularly popular in remote sensing applications as a backbone or feature extractor (Alsabhan and Alotaiby, 2022; Ghorbanzadeh et al., 2021; Li et al., 2021; Reale et al., 2022; Shabbir et al., 2021; Ullo et al., 2021; Zuo et al., 2021). A single residual unit can be defined as follows:

$$y_i = h(x_i) + F(x_i, W_i) \quad (1)$$

$$x_{i+1} = f(y_i) \quad (2)$$

whereby x_i and x_{i+1} refer to the input and output of the i th residual unit; $f(y_i)$ and $f(\cdot)$ are the activation and the residual functions, respectively; and $h(\cdot)$ is the identity mapping $h(x_i) = x_i$.

Attention mechanism

In image segmentation tasks, where capturing subtle details and spatial relationships is crucial, a deep learning model needs to focus on the most relevant information within an image. The attention mechanism, introduced by Vaswani et al. (2017), significantly

aids in this by enabling a neural network to selectively concentrate on specific parts of the input data. This mechanism assigns varying weights to input elements based on their relevance, allowing the model to highlight important details and disregard irrelevant ones (John and Zhang, 2022; Shahabi and Ghorbanzadeh, 2022). By incorporating attention mechanisms, a U-Net model becomes more adaptive and responsive to the varying significance of different image regions, enhancing segmentation accuracy. This adaptability is especially valuable when dealing with complex remote sensing datasets, enabling the U-Net to manage diverse image characteristics effectively (Li et al., 2021).

Model implementation

To develop and implement the Attention ResU-Net model specifically for our study, we employed the GeoPatch Python package (Shahabi, 2022) to preprocess the dataset. The dataset, comprising train, validation, and test areas, was divided into 256×256 patches, as illustrated in Figure 4, which displays the distribution of features extracted from the DEM. One of the critical challenges in this study was the imbalanced dataset, particularly between the Retrogressive and Rotational classes. The Retrogressive class had a significantly higher number of pixels compared to the Rotational class. To address this issue, we applied class weighting during the training process. By assigning higher weights to the minority class (Rotational), we increased the penalty for misclassifying this class, which helped the model to be more sensitive and improve its accuracy in identifying the minority class. Additionally, Attention gates (Figure 5) were added to the skip connections between the encoder and decoder, allowing the model to focus on important features and improve segmentation accuracy. The model was implemented in PyTorch with ResNet-50 as feature extractor, Adam optimizer (learning rate of 0.001), batch size of 64, and data augmentation techniques like rotation and flip to enhance generalization. Training was conducted over 1000 epochs on an NVIDIA RTX 6000 GPU. Finally, the performance of these experiments was evaluated using Precision, Recall, and F1-score metrics, focusing on both the majority (retrogressive) and minority (Rotational) classes.

Results and accuracy assessment

Model performance on training and validation dataset

The best model selection criteria were based on the highest F1-score achieved on the validation dataset.

Experiments were carried out in this study to achieve the best possible result. In the first experiment, all features were fed to the model; in the second experiment, the model was trained on each feature, and in the final experiment, all single features that had the best performance were combined as a new dataset to train the model. Figure 6 shows the loss curves for the training and validation dataset. Over the course of 1000 epochs, we selected the model with the weights and parameters that achieved the lowest validation loss.

The model's performance on the validation dataset was evaluated using the F1-score. For the Rotational landslide class, the F1-score was 0.63, while for the Retrogressive class, it was 0.85, indicating a superior prediction capability. Table 1 provides a thorough overview of the accuracy assessment for the validation dataset. Figure 7 illustrates the loss curves for the model trained on each feature. It is evident from the figure that the model achieved its best performance with the Hillshade and Slope features, while other features exhibited underfitting issues. When considering the F1-score for the validation dataset, a precision of 0.60 and 0.70 was attained for Rotational and Retrogressive classes, respectively, when the model was trained on the Hillshade feature. On the other hand, training the model on the Slope feature resulted in F1-scores of 0.62 and 0.81 for Rotational and Retrogressive classes, respectively. Conversely, the Total Curvature feature exhibited the weakest performance, with F1-scores of 0.12 for the Rotational class and 0.55 for the Retrogressive class. Table 1 details information on each feature performance based on the validation dataset. According to graphs 1 and 2 of Figure 4, the best performance was achieved using slope and hillshade features. In contrast, the total curvature offers the weakest performance in the training of the model. In the third experiment, both Hillshade and Slope were utilized as input features for the model, employing identical training parameters (Figure 8). Remarkably, the resulting F1-score values for the Rotational and Retrogressive classes were 0.71 and 0.96, respectively. This finding signifies a substantial enhancement in predictive performance, particularly for the Retrogressive class, where the achieved F1-score of 0.96 stands out prominently. Notably, the model trained on Hillshade and Slope features exhibited superior accuracy compared to other models. For instance, it achieved an impressive F1-score of 0.96 for the Retrogressive class, surpassing the maximum F1-score of 0.86 attained by the same class in other models. Table 1 presents the detailed accuracy assessments of all models using the validation dataset.

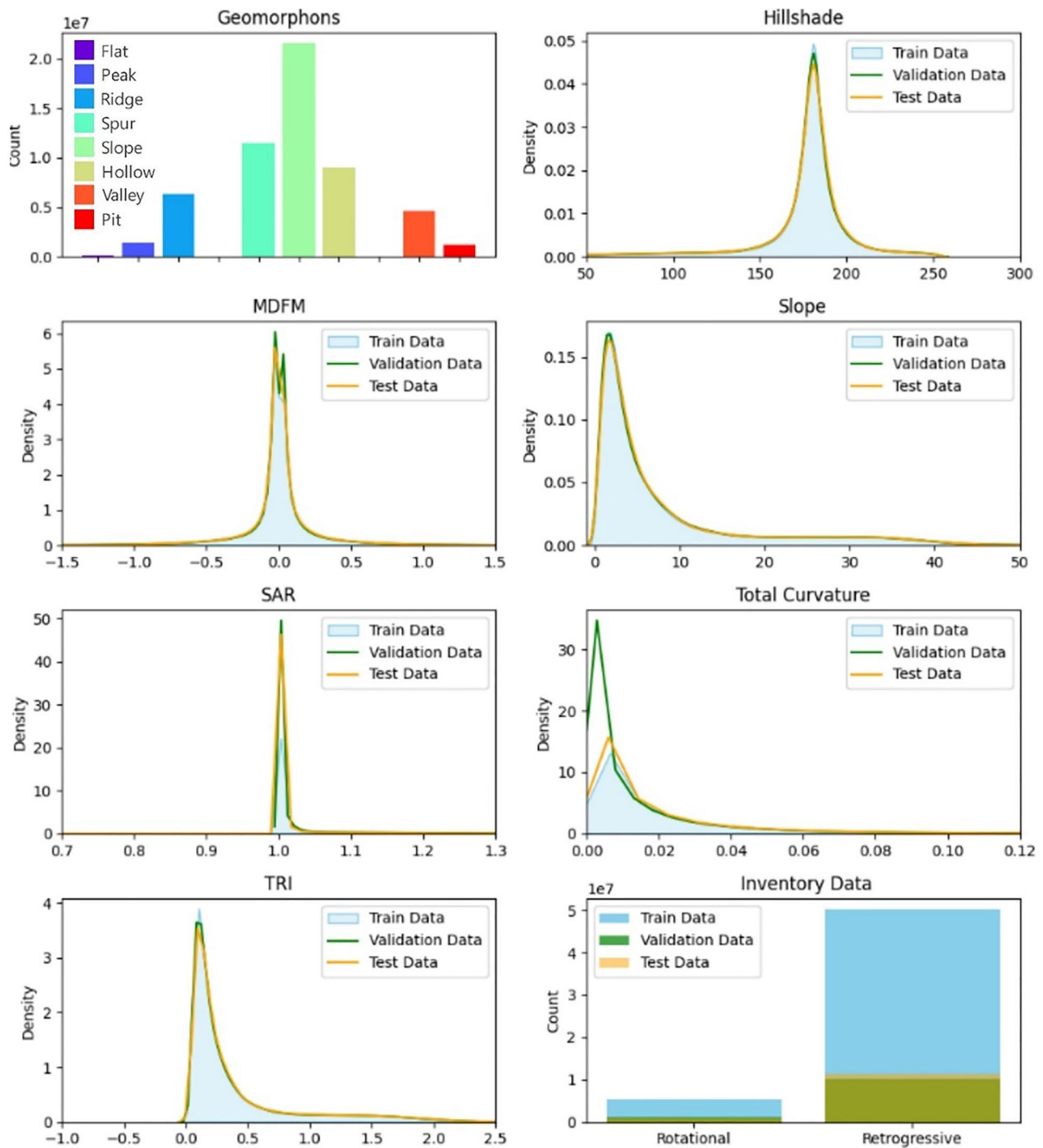


Figure 4. Visual presentation of features extracted from LiDAR data for landslide detection. Sky blue, green, and orange represent train, validation, and test data. For the geomorphons dataset (categorical), there were no features such as shoulder and footslopes. The box on the fourth row, the second column, shows the labeled pixels for Rotational and Retrogressive landslides.

Model performance on the test dataset

During the validation dataset accuracy assessment, it became evident that models trained using all features and the combination of Hillshade and Slope demonstrated the highest performance, particularly regarding the F1-score. Consequently, we exclusively employed models trained on these two datasets for the

subsequent testing phase, recognizing their superior ability to capture and utilize relevant information for landslide segmentation effectively. In comparing two scenarios of landslide segmentation using deep learning models, it is evident that focusing solely on Hillshade and Slope features yields competitive or improved results compared to utilizing all six features (Table 2). Specifically, for Rotational landslides,

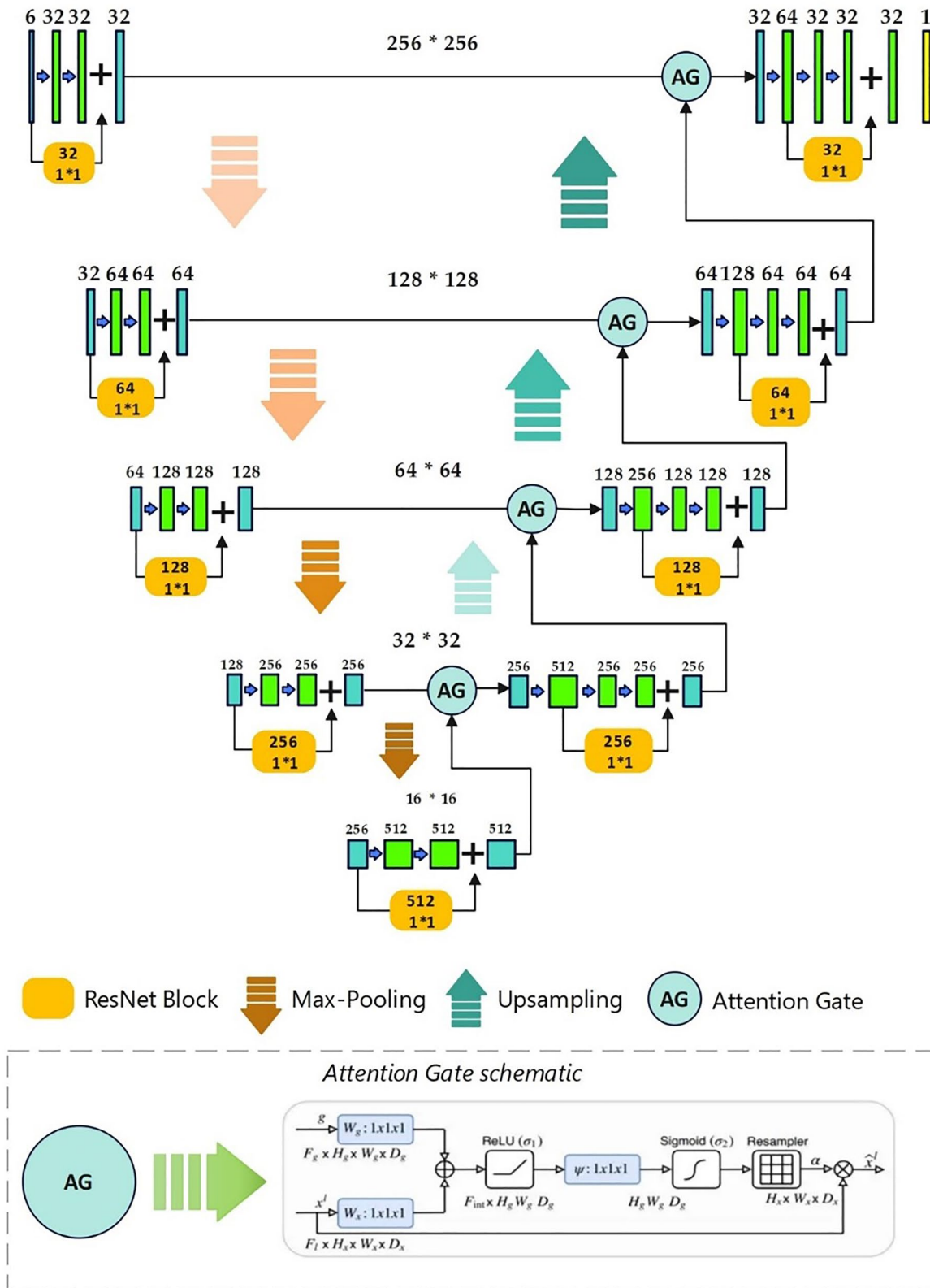


Figure 5. Graphical representation of the ResU-Net architecture with attention mechanism applied in this study.

precision (7%), recall (11%), and F1-score (7%) show improvement with the reduced feature set, suggesting that the additional features in the first scenario might introduce noise or redundancy. Furthermore, a similar

trend is observed for Retrogressive landslides; for instance, utilizing Hillshade and Slope features led to notable enhancements in metrics such as recall (16%), precision (4%), and F1-score (10%), indicating a

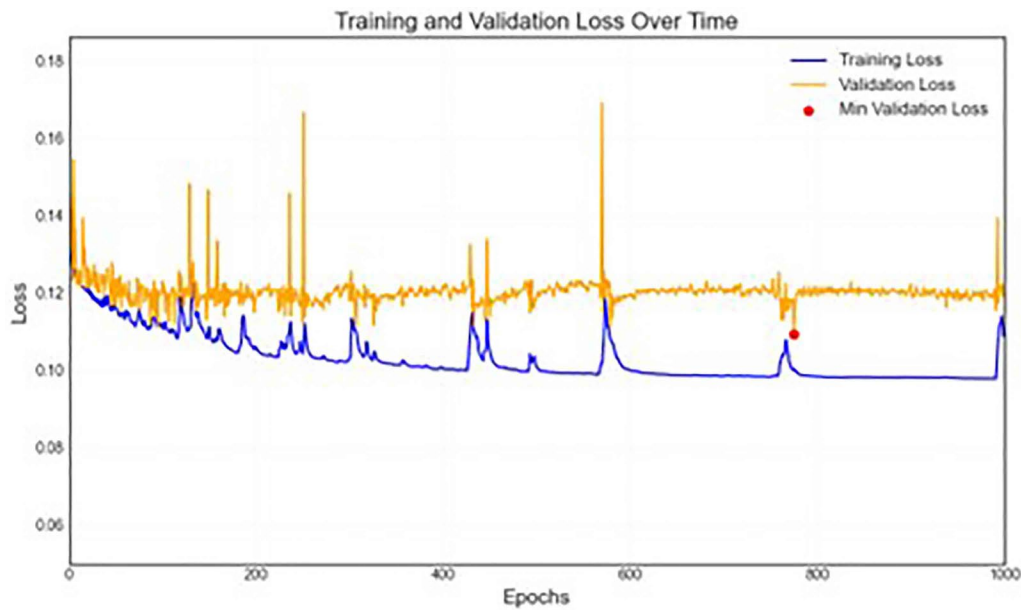


Figure 6. Loss curves for training and validation for the model training of the dataset with six features. The red dot on the graph shows the minimum loss for the validation dataset.

Table 1. Accuracy assessment metrics for trained models evaluated on the validation dataset.

Model trained on	Class	Precision	Recall	F1-score
All features	Rotational	0.6	0.67	0.63
	Retrogressive	0.82	0.89	0.85
Geomorphons	Rotational	0.1	0.91	0.18
	Retrogressive	0.72	0.55	0.63
Hillshade	Rotational	0.61	0.57	0.6
	Retrogressive	0.56	0.88	0.70
MDFM	Rotational	0.12	0.69	0.21
	Retrogressive	0.55	0.44	0.49
Slope	Rotational	0.61	0.62	0.62
	Retrogressive	0.79	0.84	0.81
SAR	Rotational	0.1	0.97	0.18
	Retrogressive	0.9	0.82	0.86
Total curvature	Rotational	0.18	0.09	0.12
	Retrogressive	0.38	0.99	0.55
TRI	Rotational	0.08	0.82	0.14
	Retrogressive	0.51	0.71	0.59
Hillshade and slope	Rotational	0.67	0.76	0.71
	Retrogressive	0.98	0.95	0.96

commendable balance between precision and recall. Finally, this implies that these two features might capture the most relevant information for accurately identifying landslides, potentially simplifying the model input and reducing computational complexity without sacrificing accuracy. Figures 9 and 10 show prediction results for Rotational and Retrogressive landslides in some random locations.

Discussion

This study explored the application of DL models, specifically ResU-Net, along with attention mechanisms, which helps the model to focus on subtle

details and spatial relationships for mapping landslides in the Quebec province using HRDEM data and its derivatives that include hill-shade, slope, total curvature, TRI, SAR, and MDFM. Three scenarios were conducted to evaluate the effectiveness of the derived features in mapping landslides. In the first scenario, all features were fed to the model. In the second scenario, training was done on all features separately, and for the final scenario, only features (hillshade and slope) with the highest performance were stacked together as the input to feed to our model. The results obtained from the model performance on both validation and test datasets provide valuable insights into the effectiveness of different features in accurately identifying landslides, such as Rotational and retrogressive. Among these features, hillshade and slope together demonstrated superior performance in capturing relevant information for landslide segmentation, as evidenced by higher F1-scores for both validation and test datasets. The precision, recall, and F1-score results indicated that focusing solely on hillshade and slope features yielded competitive or improved performance compared to utilizing all six features. This fact highlights the importance of feature selection in optimizing model performance and reducing computational complexity. The results of the experiments offer intriguing insights into the efficacy of feature selection and model performance. While DL models are renowned for their ability to extract meaningful features from raw data autonomously, the findings of this study suggest a nuanced perspective on their effectiveness in certain contexts.

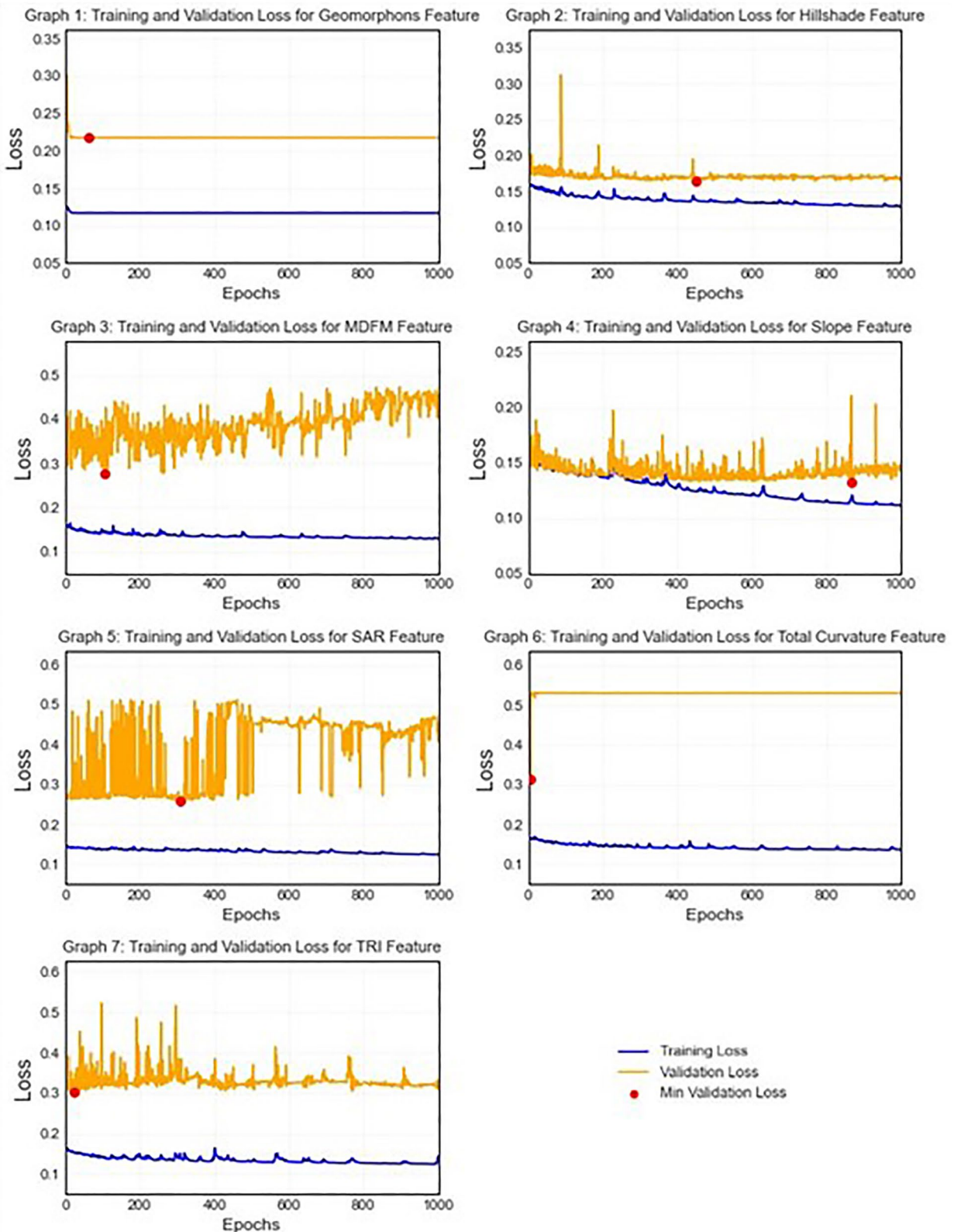


Figure 7. Training and Loss curves of the proposed model based on each feature separately.

Typically, DL models leverage their inherent capacity to discern intricate patterns and relationships within input data, making them a promising tool for tasks like landslide mapping. However, this study

presents a scenario where relying solely on the automatic extraction of features from a plethora of input data—such as hillshade, slope, total curvature, TRI, SAR, and MDFM—does not necessarily yield optimal

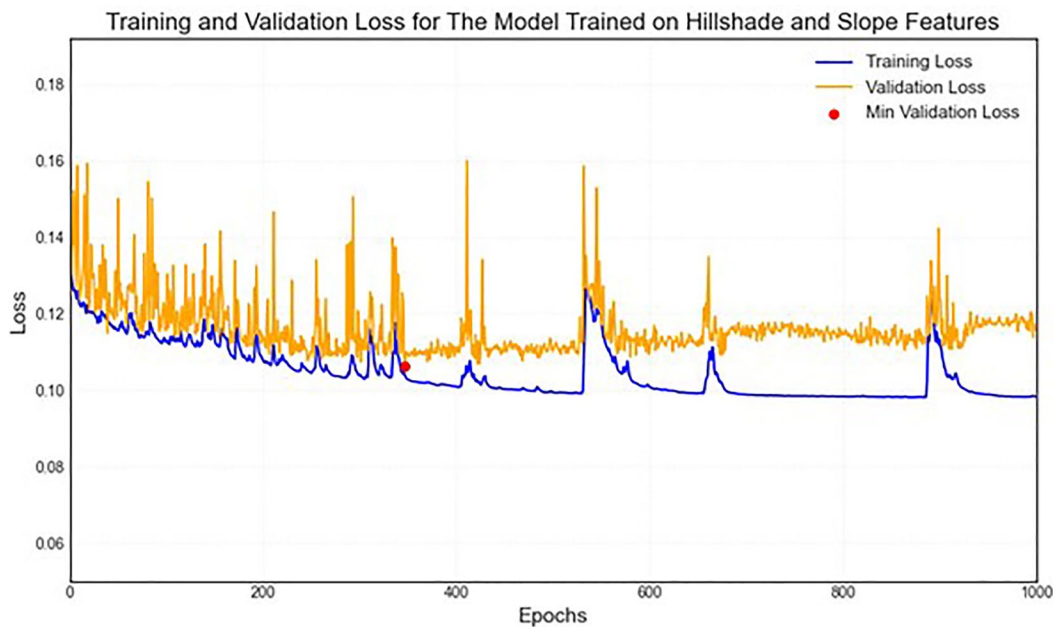


Figure 8. Training and loss curves of the trained model based on hillshade and slope features.

Table 2. Accuracy assessment metrics for the test dataset.

Model trained on	Class	Precision	Recall	F1-score
All features	Rotational	0.60	0.62	0.61
	Retrogressive	0.79	0.88	0.83
Hillshade and Slope	Rotational	0.67	0.73	0.68
	Retrogressive	0.95	0.92	0.93

results, which underscores the importance of feature selection in optimizing model performance, particularly in scenarios where certain features might overshadow or dilute the predictive power of others. The success of hillshade and slopes as discriminative features for landslide segmentation highlights their inherent relevance and significance in capturing key information in detecting landslides. Their superior performance compared to a comprehensive set of features suggests that, in this specific context, the DL model benefits more from targeted, domain-specific inputs rather than a broad array of variables. In other studies, regarding using high-resolution LiDAR data, for example, Van Den Eeckhaut et al. (2012) applied OBIA for mapping Rotational landslide in densely vegetated areas using features such as DTM, slope, plan, and profile curvature derived from LiDAR data at 2-meter resolution.

Our assessment showed they achieved 70% accuracy using image segmentation and rule-based classification. While the achieved accuracy may appear satisfactory, it is crucial to acknowledge the two significant shortcomings in their approach. Firstly, the absence of evaluation or utilization of standard methods to verify segmentation accuracy is concerning, particularly in OBIA, where incorrect segmentation

can greatly influence classification accuracy. Secondly, opting for subjective expert knowledge over an objective method, such as training a machine learning model, introduces bias. In addition, Görüm (2019) carried out the same approach for the tasks in different geographical locations. In another study, Pradhan et al. (2020) presented a novel semi-automated technique for landslide detection using Saliency Feature Enhancement (SFE) on LiDAR data. While the method offers simplicity and does not rely on extensive training datasets, its accuracy, as indicated by the prediction accuracy, falls short of providing reliable results, which needs further refinement may be necessary to enhance its reliability in practical applications. In a similar study, Fang et al. (2022) employed a lightweight attention U-Net model to map historical landslides of a single type using LiDAR data in densely vegetated mountainous regions of the Jiuzhaigou area in China. The authors trained their models on aerial images and various features derived from LiDAR data. Their accuracy assessment revealed that the RRIM (Red Relief Image Map) and hillshade data type yielded the highest performance, achieving an F1-score of 87%, surpassing optical images, raw LiDAR DEM, and hillshade derivatives.

In contrast to our study, where we addressed two types of landslides, adding complexity to the model, our dataset had a resolution of 2 meters, while theirs boasted a higher resolution of 1-meter. Additionally, our inventory data covered a wide range of slopes, whereas landslides in the Jiuzhaigou region predominantly occurred on steep slopes. Another issue we

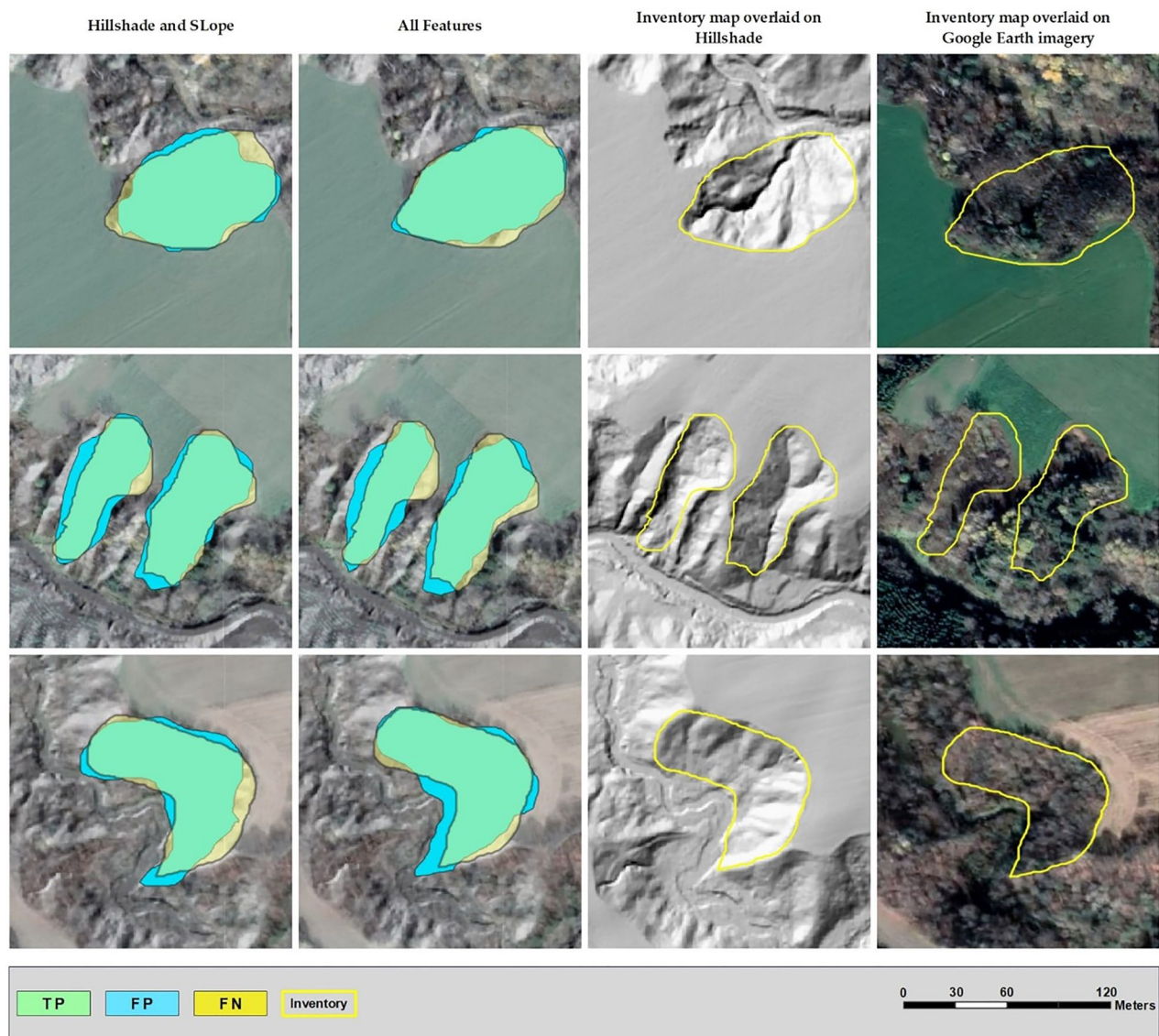


Figure 9. The prediction results for random, sometimes coalescing, Rotational landslides in the test area are depicted here. TP, FP, and FN denote true positives, false positives, and false negatives, respectively. Landslide inventory polygons are overlaid on Hillshade and Google Earth imagery to enhance the visualization.

were dealing with was the smoothing of landslide topography by earthworks. Additionally, our study contended with challenges posed by agricultural reclamation in study areas, where farmers often smooth landslide topography, complicating detection efforts. In some cases, only a subtle change in topography remains, making identifying a landslide scar particularly difficult, even for a trained eye. In addition, natural weathering processes can significantly alter landslide topography over millennia. The superior performance of hand-picked features in this study emphasizes the complementary roles of domain expertise and automated techniques in geospatial analysis. While DL models hold immense potential for feature extraction and pattern recognition, their performance

can be significantly optimized through judicious feature selection. This nuanced approach demonstrates that combining domain-specific knowledge with advanced DL techniques can lead to more robust and effective solutions in landslide mapping and beyond.

Conclusion

This study demonstrates the effectiveness of convolutional DL models, specifically ResU-Net with attention mechanisms, in mapping landslide inventory in Quebec, Canada, using HRDEM data and its derivatives. A series of experiments found that hillshade and slope features outperformed other variables in accurately identifying landslides, showcasing higher

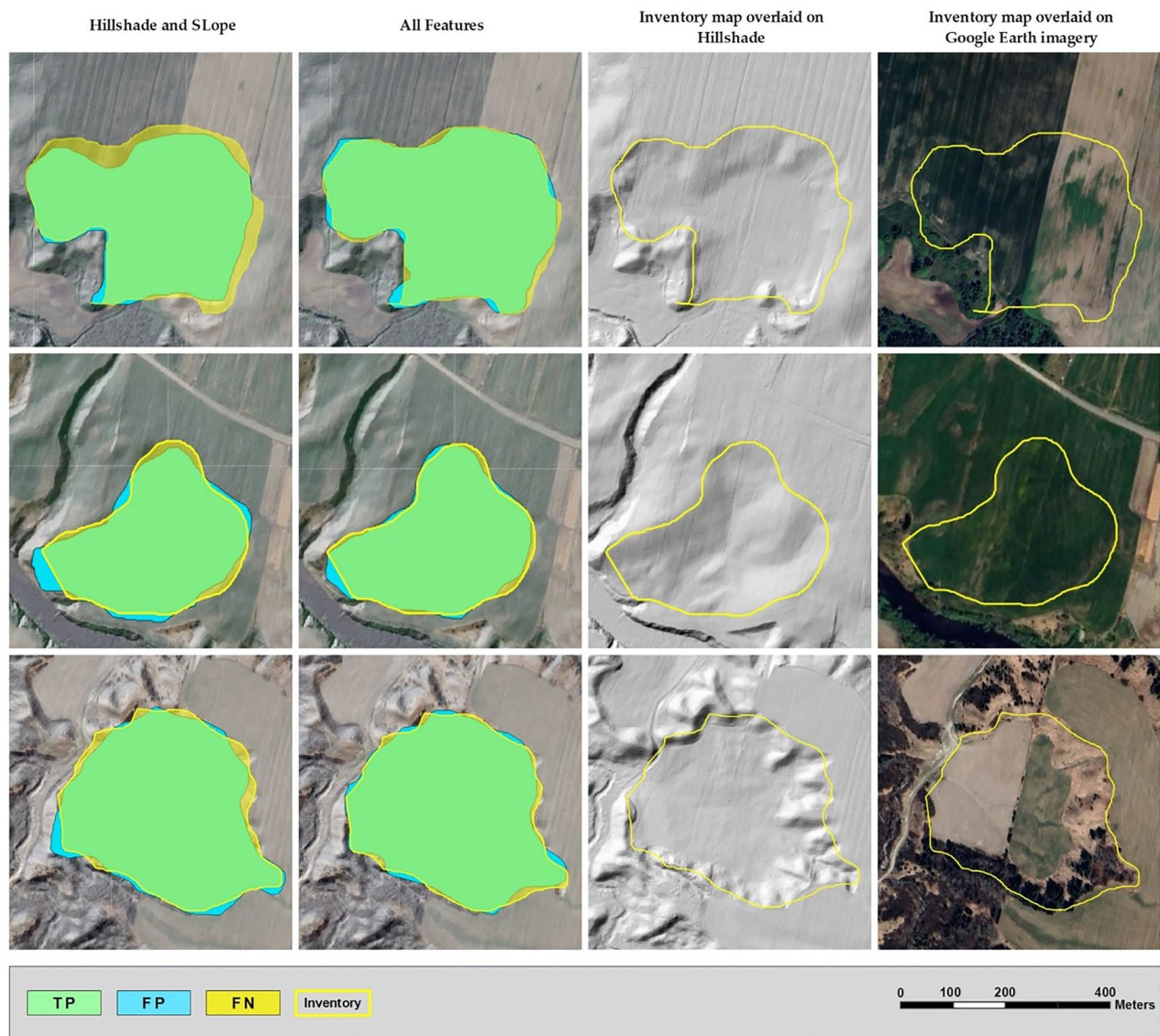


Figure 10. illustrates the prediction results for random Retrogressive landslides within the test area. The same symbols as those in Figure 9 are applicable here as well.

F1 scores and improved precision and recall metrics. Notably, focusing solely on these features yielded competitive or enhanced performance compared to utilizing all six features, emphasizing the importance of feature selection in optimizing model performance and reducing computational complexity. The study highlights the significance of targeted, domain-specific inputs in DL model training for landslide mapping tasks, offering valuable insights for future research in this field. The next phase of this research aims to enhance detection accuracy further. By incorporating high-resolution aerial images and leveraging effective features such as hillshade and slope, the authors intend to improve the precision and recall of landslide identification. Additionally, the study will explore using OBIA approach with a stronger emphasis on

better segmentation to delineate the boundaries of different landslides. This strategy is anticipated to provide more detailed and accurate mapping results, offering a promising avenue for advancing landslide inventory mapping methodologies.

Acknowledgments

I would like to acknowledge that the dataset used in this study comes from the High-Resolution Digital Elevation Model (HRDEM) product based on LiDAR data by Quebec Ministry of Natural Resources and Forests.

Disclosure statement

No potential conflict of interest was reported by the author(s).

Funding

I would like to express my sincere gratitude to the Québec Merit Scholarship Program for Foreign Students (PBEEE) for their generous financial support. This research was funded by the Fonds de recherche du Québec – Nature et technologies (FRQNT) under the award file number 352208.

References

- Aleissae, A.A., Kumar, A., Anwer, R.M., Khan, S., Cholakkal, H., Xia, G.-S., and Khan, F.S. 2023. “Transformers in remote sensing: A survey.” *Remote Sensing*, Vol. 15 (No. 7): pp. 1860. doi:10.3390/rs15071860.
- Alsabhan, W., and Alotaiby, T. 2022. “Automatic building extraction on satellite images using Unet and ResNet50.” *Computational Intelligence and Neuroscience*, Vol. 2022 (No. 1): pp. 5008854. doi:10.1155/2022/5008854.
- Azañón, J.M., Azor, A., Pérez-Peña, J.V., and Carrillo, J.M. 2005. “Late quaternary large-scale rotational slides induced by river incision: The Arroyo de Gor area (Guadix Basin, SE Spain).” *Geomorphology*, Vol. 69 (No. 1-4): pp. 152–168. doi:10.1016/j.geomorph.2004.12.007.
- Azhand, D., Pirasteh, S., Varshosaz, M., Shahabi, H., Abdollahabadi, S., Teimouri, H., Pirnazar, M., Wang, X., and Li, W. 2024. “Sentinel 1a-2a incorporating an object-based image analysis method for flood mapping and extent assessment.” *ISPRS Annals of the Photogrammetry, Remote Sensing and Spatial Information Sciences*, Vol. X-1-2024: pp. 7–17. doi:10.5194/isprs-annals-X-1-2024-7-2024.
- Blais-Stevens, A., Behnia, P., and Castagner, A. 2018. “Historical landslides that have resulted in fatalities in Canada (1771–2018).” *Open File*, pp. 8392.
- Chapuis, R. 2016. “Extracting information from grain size distribution curves.” *Geotechnical News*, Vol. 37: pp. 1–2.
- Chen, W., Li, X., Wang, Y., Chen, G., and Liu, S. 2014. “Forested landslide detection using LiDAR data and the random forest algorithm: A case study of the Three Gorges, China.” *Remote Sensing of Environment*, Vol. 152: pp. 291–301. doi:10.1016/j.rse.2014.07.004.
- Demers, D., Robitaille, D., Lavoie, A., Paradis, S., Fortin, A., and Ouellet, D. 2017. “The use of LiDAR airborne data for Retrogressive landslides inventory in sensitive clays, Québec, Canada.” In *Landslides in Sensitive Clays*, edited by V. Thakur, JS. L’Heureux, A. Locat. Advances in Natural and Technological Hazards Research, vol 46. Cham: Springer. doi:10.1007/978-3-319-56487-6_25.
- Demers, D., Robitaille, D., Locat, P., and Potvin, J. 2014. “Inventory of large landslides in sensitive clay in the province of Québec, Canada: preliminary analysis.” In *Landslides in Sensitive Clays: From Geosciences to Risk Management*, 77–89.
- Fang, C., Fan, X., Zhong, H., Lombardo, L., Tanyas, H., and Wang, X. 2022. “A novel historical landslide detection approach based on LiDAR and lightweight attention U-Net.” *Remote Sensing*, Vol. 14 (No. 17): pp. 4357. doi:10.3390/rs14174357.
- Florinsky, I. 2016. *Digital Terrain Analysis in Soil Science and Geology*. London: Elsevier.
- Gallant, J. C. 2000. “Primary topographic attributes.” In *Terrain Analysis-Principles and Application*, edited by John P. Wilson, and John C. Gallant, 51–86. USA: John Wiley & Sons.
- Ghorbanzadeh, O., Crivellari, A., Ghamisi, P., Shahabi, H., and Blaschke, T. 2021. “A comprehensive transferability evaluation of U-Net and ResU-Net for landslide detection from Sentinel-2 data (case study areas from Taiwan, China, and Japan).” *Scientific Reports*, Vol. 11 (No. 1): pp. 1–20. doi:10.1038/s41598-021-94190-9.
- Ghorbanzadeh, O., Gholamnia, K., and Ghamisi, P. 2023. “The application of ResU-net and OBIA for landslide detection from multi-temporal sentinel-2 images.” *Big Earth Data*, Vol. 7 (No. 4): pp. 961–985. doi:10.1080/20964471.2022.2031544.
- Ghorbanzadeh, O., Shahabi, H., Crivellari, A., Homayouni, S., Blaschke, T., and Ghamisi, P. 2022. “Landslide detection using deep learning and object-based image analysis.” *Landslides*, Vol. 19 (No. 4): pp. 929–939. doi:10.1007/s10346-021-01843-x.
- Ghorbanzadeh, O., Shahabi, H., Piralilou, S.T., Crivellari, A., La Rosa, L.E.C., Atzberger, C., Li, J., and Ghamisi, P. 2024. “Contrastive Self-Supervised Learning for Globally Distributed Landslide Detection.” *IEEE Access*, Vol. 12: pp. 118453–118466. doi:10.1109/ACCESS.2024.3449447.
- Görüm, T. 2019. “Landslide recognition and mapping in a mixed forest environment from airborne LiDAR data.” *Engineering Geology*, Vol. 258: pp. 105155. doi:10.1016/j.enggeo.2019.105155.
- Guzzetti, F. 2000. “Landslide fatalities and the evaluation of landslide risk in Italy.” *Engineering Geology*, Vol. 58 (No. 2): pp. 89–107. doi:10.1016/S0013-7952(00)00047-8.
- Guzzetti, F., Mondini, A.C., Cardinali, M., Fiorucci, F., Santangelo, M., and Chang, K.-T. 2012. “Landslide inventory maps: New tools for an old problem.” *Earth-Science Reviews*, Vol. 112 (No. 1-2): pp. 42–66. doi:10.1016/j.earscirev.2012.02.001.
- He, K., Gkioxari, G., Dollár, P., and Girshick, R. 2017. “Mask r-cnn.” In *Proceedings of the IEEE international conference on computer vision*, 2961–2969.
- He, K., Zhang, X., Ren, S., and Sun, J. 2016. “Deep residual learning for image recognition.” Paper presented at *Proceedings of the IEEE conference on computer vision and pattern recognition*, 770–778.
- Hölbling, D., Betts, H., Spiekermann, R., and Phillips, C. 2016. “Identifying spatio-temporal landslide hotspots on North Island, New Zealand, by analyzing historical and recent aerial photography.” *Geosciences*, Vol. 6 (No. 4): pp. 48. doi:10.3390/geosciences6040048.
- Hölbling, D., Friedl, B., and Eisank, C. 2015. “An object-based approach for semi-automated landslide change detection and attribution of changes to landslide classes in northern Taiwan.” *Earth Science Informatics*, Vol. 8 (No. 2): pp. 327–335. doi:10.1007/s12145-015-0217-3.
- Jasiewicz, J., and Stepinski, T.F. 2013. “Geomorphons—A pattern recognition approach to classification and mapping of landforms.” *Geomorphology*, Vol. 182: pp. 147–156. doi:10.1016/j.geomorph.2012.11.005.
- Jenness, J.S. 2004. “Calculating landscape surface area from digital elevation models.” *Wildlife Society Bulletin*, Vol. 32 (No. 3): pp. 829–839. doi:10.2193/0091-7648(2004)032[0829:CLSAFD]2.0.CO;2.
- John, D., and Zhang, C. 2022. “An attention-based U-Net for detecting deforestation within satellite sensor imagery.” *International Journal of Applied Earth Observation*

- and *Geoinformation*, Vol. 107: pp. 102685. doi:10.1016/j.jag.2022.102685.
- Ju, Y., Xu, Q., Jin, S., Li, W., Su, Y., Dong, X., and Guo, Q. 2022. "Loess landslide detection using object detection algorithms in Northwest China." *Remote Sensing*, Vol. 14 (No. 5): pp. 1182. doi:10.3390/rs14051182.
- Kariminejad, N., Shahabi, H., Ghorbanzadeh, O., Shafaie, V., Hosseinalzadeh, M., Homayouni, S., and Pourghasemi, H.R. 2024. "Evaluation of various deep learning algorithms for landslide and sinkhole detection from UAV imagery in a semi-arid environment." *Earth Systems and Environment*, pp. 1–12. doi:10.1007/s41748-024-00419-8.
- Keyport, R.N., Oommen, T., Martha, T.R., Sajinkumar, K.S., and Gierke, J.S. 2018. "A comparative analysis of pixel- and object-based detection of landslides from very high-resolution images." *International Journal of Applied Earth Observation and Geoinformation*, Vol. 64: pp. 1–11. doi:10.1016/j.jag.2017.08.015.
- L'Heureux, J.S., Locat, A., Leroueil, S., Demers, D., Locat, J. (2014). Landslides in Sensitive Clays – From Geosciences to Risk Management. In *Landslides in Sensitive Clays*, edited by L'Heureux, J.S., Locat, A., Leroueil, S., Demers, D., Locat, J. Advances in Natural and Technological Hazards Research, Vol. 36. Dordrecht: Springer. doi:10.1007/978-94-007-7079-9_1
- Li, R., Zheng, S., Zhang, C., Duan, C., Su, J., Wang, L., and Atkinson, P.M. 2021. "Multiattention network for semantic segmentation of fine-resolution remote sensing images." *IEEE Transactions on Geoscience and Remote Sensing*, Vol. 60: pp. 1–13. doi:10.1109/TGRS.2021.3093977.
- Li, X., Cheng, X., Chen, W., Chen, G., and Liu, S. 2015. "Identification of forested landslides using LiDAR data, object-based image analysis, and machine learning algorithms." *Remote Sensing*, Vol. 7 (No. 8): pp. 9705–9726. doi:10.3390/rs70809705.
- Lindsay, J. B. 2005. "The terrain analysis system: A tool for hydro-geomorphic applications." *Hydrological Processes*, Vol. 19 (No. 5): pp. 1123–1130.
- Locat, A., Leroueil, S., Bernander, S., Demers, D., Pette Jostad, H., and Ouehb, L. 2011. "Progressive failures in eastern Canadian and Scandinavian sensitive clays." *Canadian Geotechnical Journal*, Vol. 48 (No. 11): pp. 1696–1712. doi:10.1139/t11-059.
- Lu, W., Hu, Y., Zhang, Z., and Cao, W. 2023. "A dual-encoder U-Net for landslide detection using Sentinel-2 and DEM data." *Landslides*, Vol. 20 (No. 9): pp. 1975–1987. doi:10.1007/s10346-023-02089-5.
- Ma, L., Liu, Y., Zhang, X., Ye, Y., Yin, G., and Johnson, B.A. 2019. "Deep learning in remote sensing applications: A meta-analysis and review." *ISPRS Journal of Photogrammetry and Remote Sensing*, Vol. 152: pp. 166–177. doi:10.1016/j.isprsjprs.2019.04.015.
- Ma, S., Qiu, H., Zhu, Y., Yang, D., Tang, B., Wang, D., Wang, L., and Cao, M. 2023. "Topographic changes, surface deformation and movement process before, during and after a Rotational landslide." *Remote Sensing*, Vol. 15 (No. 3): pp. 662. doi:10.3390/rs15030662.
- Maggiore, Emmanuel., Tarabalka, Yuliya., Charpiat, Guillaume., and Alliez, Pierre 2016. "Fully convolutional neural networks for remote sensing image classification." In *2016 IEEE international geoscience and remote sensing symposium (IGARSS)*, 5071–5074. Beijing: IEEE.
- Mezaal, M.R., Pradhan, B., and Rizeei, H.M. 2018. "Improving landslide detection from airborne laser scanning data using optimized Dempster–Shafer." *Remote Sensing*, Vol. 10 (No. 7): pp. 1029. doi:10.3390/rs10071029.
- Mohan, A., Kumar Singh, A., Kumar, B., and Dwivedi, R. 2021. "Review on remote sensing methods for landslide detection using machine and deep learning." *Transactions on Emerging Telecommunications Technologies*, Vol. 32 (No. 7): pp. e3998. doi:10.1002/ett.3998.
- Natural Resources Canada. 2019. "High resolution digital elevation model (HRDEM)—CanElevation Series—Product specifications."
- Pawłuszek, K., Marczak, S., Borkowski, A., and Tarolli, P. 2019. "Multi-aspect analysis of object-oriented landslide detection based on an extended set of LiDAR-derived terrain features." *ISPRS International Journal of Geo-Information*, Vol. 8 (No. 8): pp. 321. doi:10.3390/ijgi8080321.
- Perret, Didier., Therrien, Julie., Locat, Pascal., and Demers, Denis 2019. "Influence of surficial crusts on the development of spreads and flows in Eastern Canadian sensitive clays." In *72th Canadian Geotechnical Conference (GeoSt. Johns2019)*, St. John's, Newfoundland & Labrador, Canada, September–October 2019.
- Poulin Leboeuf, L. 2020. "Analyse statistique des facteurs climatiques et géomorphologiques associés aux mouvements de terrain dans les argiles des mers post-glaciaires au Québec méridional (Master's thesis)." Université Laval, Faculté de foresterie, de géographie et de géomatique. Retrieved from <https://dam-oclc.bac-lac.gc.ca/eng/c1284a17-be4a-49cd-8fbf-2876c8909f2d>
- Pradhan, B., Al-Najjar, H.A.H., Sameen, M.I., Mezaal, M.R., and Alamri, A.M. 2020. "Landslide detection using a saliency feature enhancement technique from LiDAR-derived DEM and orthophotos." *IEEE Access*, Vol. 8: pp. 121942–121954. doi:10.1109/ACCESS.2020.3006914.
- Prakash, N., Manconi, A., and Loew, S. 2020. "Mapping landslides on EO data: Performance of deep learning models vs. traditional machine learning models." *Remote Sensing*, Vol. 12 (No. 3): pp. 346. doi:10.3390/rs12030346.
- Reale, D., Verde, S., Calà, F., Imperatore, P., Pauciullo, A., Pepe, A., Zamparelli, V., Sansosti, E., and Fornaro, G. 2022. "Multipass InSAR with multiple bands: Application to landslides mapping and monitoring." In *IGARSS 2022-2022 IEEE International Geoscience and Remote Sensing Symposium*, 4510–13. Kuala Lumpur: IEEE.
- Ronneberger, Olaf., Fischer, Philipp., and Brox, Thomas 2015. "U-net: Convolutional networks for biomedical image segmentation." In *International Conference on Medical image computing and computer-assisted intervention*, 234–241. Cham: Springer.
- Saba, S.B., Ali, M., Ali Turab, S., Waseem, M., and Faisal, S. 2023. "Comparison of pixel, sub-pixel and object-based image analysis techniques for co-seismic landslides detection in seismically active area in Lesser Himalaya, Pakistan." *Natural Hazards*, Vol. 115 (No. 3): pp. 2383–2398. doi:10.1007/s11069-022-05642-y.
- Shabbir, A., Ali, N., Ahmed, J., Zafar, B., Rasheed, A., and Sajid, M. 2021. "Afzal Ahmed, and Saadat Hanif Dar. 2021. 'Satellite and scene image classification based on transfer learning and fine tuning of ResNet50.' *Mathematical Problems in Engineering*, pp. 1–18.
- Shahabi, Hejar. 2022. "GeoPatch is a package for generating patches from remote sensing data." <https://pypi.org/>.

- Shahabi, H., and Ghorbanzadeh, O. 2022. "Model-centric vs data-centric deep learning approaches for landslide detection." In CDCEO 2022: 2nd Workshop on Complex Data Challenges in Earth Observation, Vienna, Austria.
- Shahabi, H., Ghorbanzadeh, O., Homayouni, S., and Ghamisi, P. 2024. "A comparison of SimCLR and SwAV contrastive self-supervised learning models for landslide detection, EGU General Assembly 2024, Vienna, Austria." doi: [10.5194/egusphere-egu24-4772](https://doi.org/10.5194/egusphere-egu24-4772).
- Shahabi, H., Jarihani, B., Tavakkoli Piralilou, S., Chittleborough, D., Avand, M., and Ghorbanzadeh, O. 2019. "A semi-automated object-based gully networks detection using different machine learning models: a case study of Bowen catchment, Queensland, Australia." *Sensors*, Vol. 19 (No. 22): pp. 4893. doi:[10.3390/s19224893](https://doi.org/10.3390/s19224893).
- Shahabi, H., Rahimzad, M., Tavakkoli Piralilou, S., Ghorbanzadeh, O., Homayouni, S., Blaschke, T., Lim, S., and Ghamisi, P. 2021. "Unsupervised deep learning for landslide detection from multispectral sentinel-2 imagery." *Remote Sensing*, Vol. 13 (No. 22): pp. 4698. doi:[10.3390/rs13224698](https://doi.org/10.3390/rs13224698).
- Shih, H.-c., Stow, D.A., and Tsai, Y.H. 2019. "Guidance on and comparison of machine learning classifiers for landsat-based land cover and land use mapping." *International Journal of Remote Sensing*, Vol. 40 (No. 4): pp. 1248–1274. doi:[10.1080/01431161.2018.1524179](https://doi.org/10.1080/01431161.2018.1524179).
- Su, Z., Li, W., Ma, Z., and Gao, R. 2022. "An improved U-Net method for the semantic segmentation of remote sensing images." *Applied Intelligence*, Vol. 52 (No. 3): pp. 3276–3288. doi:[10.1007/s10489-021-02542-9](https://doi.org/10.1007/s10489-021-02542-9).
- Tanatipuknon, A., Aimmanee, P., Watanabe, Y., Murata, K.T., Wakai, A., Sato, G., Hung, H.V., Tungpimolrut, K., Keerativittayanun, S., and Karnjana, J, Sirindhorn International Institute of Technology, Thammasat University Pathum Thani, Thailand 2021. "Study on combining two faster R-CNN models for landslide detection with a classification decision tree to improve the detection performance." *Journal of Disaster Research*, Vol. 16 (No. 4): pp. 588–595. doi:[10.20965/jdr.2021.p0588](https://doi.org/10.20965/jdr.2021.p0588).
- Tang, X., Tu, Z., Wang, Y., Liu, M., Li, D., and Fan, X. 2022. "Automatic detection of Coseismic landslides using a new transformer method." *Remote Sensing*, Vol. 14 (No. 12): pp. 2884. doi:[10.3390/rs14122884](https://doi.org/10.3390/rs14122884).
- Tavakkoli Piralilou, S., Shahabi, H., Jarihani, B., Ghorbanzadeh, O., Blaschke, T., Gholamnia, K., Raj Meena, S., and Aryal, J. 2019. "Landslide detection using multi-scale image segmentation and different machine learning models in the higher Himalayas." *Remote Sensing*, Vol. 11 (No. 21): pp. 2575. doi:[10.3390/rs11212575](https://doi.org/10.3390/rs11212575).
- Ullo, S., Mohan, A., Sebastianelli, A., Ahamed, S., Kumar, B., Dwivedi, R., and Sinha, G.R. 2021. "A new mask R-CNN-based method for improved landslide detection." *IEEE Journal of Selected Topics in Applied Earth Observations and Remote Sensing*, Vol. 14: pp. 3799–3810. doi:[10.1109/JSTARS.2021.3064981](https://doi.org/10.1109/JSTARS.2021.3064981).
- Van Den Eeckhaut, M., Kerle, N., Poesen, J., and Hervás, J. 2012. "Object-oriented identification of forested landslides with derivatives of single pulse LiDAR data." *Geomorphology*, Vol. 173–174: pp. 30–42. doi:[10.1016/j.geomorph.2012.05.024](https://doi.org/10.1016/j.geomorph.2012.05.024).
- Varnes, D.J. 1978. "Slope movement types and processes." *Special Report*, Vol. 176: pp. 11–33.
- Vaswani, A., Shazeer, N., Parmar, N., Uszkoreit, J., Jones, L., Gomez, A.N., Kaiser, Ł., and Polosukhin, I. 2017. "Attention is all you need." *Advances in Neural Information Processing Systems*, Vol. 30: pp. 1–15.
- Wang, Z., Sun, T., Hu, K., Zhang, Y., Yu, X., and Li, Y. 2022. "A Deep Learning Semantic Segmentation Method for Landslide Scene Based on Transformer Architecture." *Sustainability*, Vol. 14 (No. 23): pp. 16311. doi:[10.3390/su142316311](https://doi.org/10.3390/su142316311).
- Yang, Z., Xu, C., and Li, L. 2022. "Landslide Detection Based on ResU-Net with Transformer and CBAM Embedded: Two Examples with Geologically Different Environments." *Remote Sensing*, Vol. 14 (No. 12): pp. 2885. doi:[10.3390/rs14122885](https://doi.org/10.3390/rs14122885).
- Zhang, Z., Liu, Q., and Wang, Y. 2018. "Road extraction by deep residual u-net." *IEEE Geoscience and Remote Sensing Letters*, Vol. 15 (No. 5): pp. 749–753. doi:[10.1109/LGRS.2018.2802944](https://doi.org/10.1109/LGRS.2018.2802944).
- Zuo, R., Zhang, G., Zhang, R., and Jia, X. 2021. "A deformable attention network for high-resolution remote sensing images semantic segmentation." *IEEE Transactions on Geoscience and Remote Sensing*, Vol. 60: pp. 1–14. doi:[10.1109/TGRS.2021.3119537](https://doi.org/10.1109/TGRS.2021.3119537).